CARBON
IN CATALYSIS

Synthesis of Nitrogen-Containing Carbon Materials for Solid Polymer Fuel Cell Cathodes

Z. R. Ismagilov[a], A. E. Shalagina[a], O. Yu. Pod''yacheva[a], Ch. N. Barnakov[b], A. P. Kozlov[b], R. I. Kvon[a], I. Z. Ismagilov[a], and M. A. Kerzhentsev[a]

[a] *Boreskov Institute of Catalysis, Siberian Branch, Russian Academy of Sciences, Novosibirsk, 630090 Russia*
[b] *Institute of Carbon and Carbon Chemistry, Siberian Branch, Russian Academy of Sciences, Kemerovo, 650099 Russia*
e-mail: zri@catalysis.ru
Received December 5, 2006

Abstract—The following nitrogen-containing supports with various nitrogen contents and structure and texture properties were synthesized: carbon nanofibers (N-CNFs) and amorphous microporous carbon materials (N-AMCMs). It was found that the above characteristics can be regulated by varying synthesis conditions: precursor compositions and reaction temperature and time. Mesoporous nitrogen-containing CNFs with a specific surface area of 30–350 m^2/g and a pore volume of 0.10–0.83 cm^3/g were formed by the catalytic decomposition of a mixture of ethylene with ammonia at 450–675°C. Microporous materials (N-AMCMs) with a specific surface area of 472–3436 m^2/g and a micropore volume of 0.22–1.88 cm^3/g were prepared by the carbonization of nitrogen-containing organic compounds at 700–900°C. An increase in the carbonization temperature and reaction time resulted in an increase in the specific surface area and microporosity of N-AMCMs, whereas lower temperatures of 450–550°C and reaction times of 1–3 h were optimal for the preparation of N-CNFs with a developed texture. It was found that milder synthesis conditions and higher nitrogen contents of precursors were required for obtaining high nitrogen concentrations in both N-CNFs and N-AMCMs. The synthetic method developed allowed us to prepare carbon supports with nitrogen contents to 8 wt %.

DOI: 10.1134/S0023158407040179

INTRODUCTION

Platinum and platinum alloys supported on carbon materials are in current use as electrocatalysts in solid polymer fuel cell cathodes [1, 2]. The efficiency of these catalysts essentially depends on the specific surface area, pore structure, electric conductivity, and other characteristics of the carbon support [3, 4]. Carbon nanofibers (CNFs) have attracted considerable attention from the standpoint of the target-oriented synthesis of an optimum support for electrocatalysts [3–8]. CNFs are formed in the decomposition of carbon-containing compounds on iron subgroup metals; these are mesoporous materials with a specific surface area of 100–300 m^2/g. It is well known [9–14] that the structure and texture properties of CNFs depend on synthesis conditions such as the composition of the catalyst, the nature of the carbon precursor, and the temperature of the process. CNFs of a certain structure and morphology can be prepared by controlling the above parameters. It was found experimentally that the use of CNFs increased the activity and stability of platinum catalysts in electrode processes and increased the platinum efficiency, as compared with commercial carbon supports [3, 5–8].

The previously developed amorphous microporous carbon materials (AMCMs) with a high specific surface area (to 3300 m^2/g) and a considerable micropore volume (to 2 cm^3/g) [15–17] belong to another type of carbon supports that can be successfully used for the manufacture of highly active electrocatalysts. Previously [8, 18], we found that AMCMs can be efficiently used as the supports of platinum catalysts based on the stabilization of highly dispersed platinum particles in micropores.

Nitrogen-containing CNFs and AMCMs (N-CNFs and N-AMCMs, respectively) are promising materials for use as the supports of cathode catalysts. The presence of specific adsorption sites on the surface of nitrogen-containing materials results in a more uniform distribution of the active component and a high dispersion and high specific surface area of Pt particles [6, 9, 19]. In addition, an increased electric conductivity of N-CNFs, as compared with that of unmodified materials [20, 21], also facilitates high electrocatalytic activity.

The attractiveness of nitrogen-containing supports is due to the necessity of synthesizing new electrocatalysts with reduced noble metal concentrations and with the replacement of noble metals by Fe and Co compounds, in particular, based on Fe and Co complexes with ligands like phthalocyanines (N_4–M complexes, where M = Fe or Co) [22–28]. These metal chelates adsorbed on a carbon support after appropriate thermal treatment are active in the reaction of oxygen reduction in an acidic medium, and nitrogen-containing func-
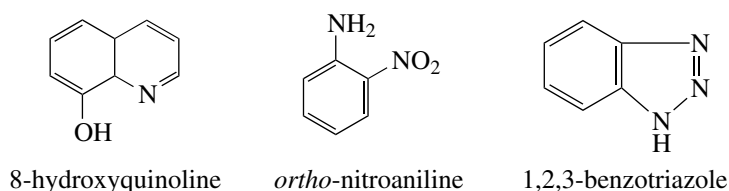
8-hydroxyquinoline　　　*ortho*-nitroaniline　　　1,2,3-benzotriazole

Fig. 1. Nitrogen-containing organic precursors of N-AMCMs.

tional groups on the support surface can serve as transition metal adsorption and stabilization sites [29]. The activity of these catalysts increases with nitrogen concentration on the surface of the carbon material. As found using X-ray photoelectron spectroscopy (XPS) [29, 30], nitrogen atoms should occur in a pyridinic state in order to form an active site. Therefore, the electronic state of nitrogen atoms on the surface of a carbon support and the possibility of regulating this state by a controllable synthesis are of considerable importance.

The aim of this work was to synthesize carbon materials structurally modified with nitrogen atoms, to study the physical chemistry of formation of nitrogen-containing carbon materials, to optimize conditions for the preparation of materials with high specific surface areas and high nitrogen contents, and to determine the state distribution of nitrogen atoms depending on synthesis conditions.

Table 1. Effect of the chemical composition of the catalyst on the yield of N-CNFs (G), the nitrogen content of the material (N), and the specific surface area (S_{BET})

Catalyst	T, °C	G, g_C/g_{Cat}	N, wt %	S_{BET}, m²/g
90Ni-Al$_2$O$_3$	550	11.6	0.47	158
82Ni-8Cu-Al$_2$O$_3$		11.5	0.90	206
65Ni-25Cu-Al$_2$O$_3$		12.4	1.58	282
45Ni-45Cu-Al$_2$O$_3$		11.2	0.74	280
72Co-3Mo-Al$_2$O$_3$	600	14.3	0.65	223
75Co-Al$_2$O$_3$		12.2	0.68	205
65Ni-25Cu-Al$_2$O$_3$		13.1	1.07	231
85Fe-5Co-Al$_2$O$_3$	625	0.5	–	–
62Fe-8Co-Al$_2$O$_3$		1.1	2.00	117
65Ni-25Cu-Al$_2$O$_3$		14.5	0.96	244

Note: Reaction conditions: decomposition of a mixture of 75% C$_2$H$_4$ and 25% NH$_3$ for 1 h.

EXPERIMENTAL

Synthesis of Nitrogen-Containing Carbon Materials

The N-CNFs were prepared by the decomposition of a mixture of C$_2$H$_4$ and NH$_3$ on the high-percentage metal catalysts[1]: 90Ni–Al$_2$O$_3$, 82Ni–8Cu–Al$_2$O$_3$, 65Ni–25Cu–Al$_2$O$_3$, 45Ni–45Cu–Al$_2$O$_3$, 85Fe–5Co–Al$_2$O$_3$, 62Fe–8Co–Al$_2$O$_3$, 75Co–Al$_2$O$_3$, and 72Co–3Mo–Al$_2$O$_3$. These catalysts were prepared by the coprecipitation of an active component and a support from a nitrate salt solution in accordance with published procedures [11, 31]. The mixtures of C$_2$H$_4$ and NH$_3$ with ammonia concentrations of 25, 50, and 75 vol % were used for the synthesis of the N-CNFs. The decomposition reaction was performed in a flow setup with a quartz vibrofluidized-bed reactor at 450–675°C and a pressure of 1 bar for 0.25–20 h. The catalyst load was 0.1 g; the flow rate of the reaction mixture was 2.25 l/h. The yield of carbon (G, g_C/g_{Cat}) was calculated as the weight ratio between the resulting carbon and the initial catalyst.

The N-AMCMs were prepared from nitrogen-containing organic precursors, which were either individual substances (8-hydroxyquinoline, *ortho*-nitroaniline, and 1,2,3-benzotriazole) or their equimolar mixtures (Fig. 1). The use of the equimolar mixtures of various nitrogen-containing organic compounds allowed us to obtain N-AMCMs with high nitrogen contents and high specific surface areas. To prepare N-AMCMs, the precursors were mixed with a concentrated aqueous solution of NaOH in a NaOH-to-precursor ratio of 1 : 3. The melt of an organic precursor with the alkali, which was obtained by the evaporation of water, was subjected to thermal treatment (carbonization) at 700–900°C for 20–80 min in a reducing atmosphere formed by carbonization gases or in an inert atmosphere. The carbonization product was washed with an aqueous solution of hydrochloric acid and then with water to a neutral reaction. The residue was dried at 105–115°C to constant weight.

[1] Henceforth, the number before the symbol of an element refers to the weight concentration in the catalyst with the balance aluminum oxide.
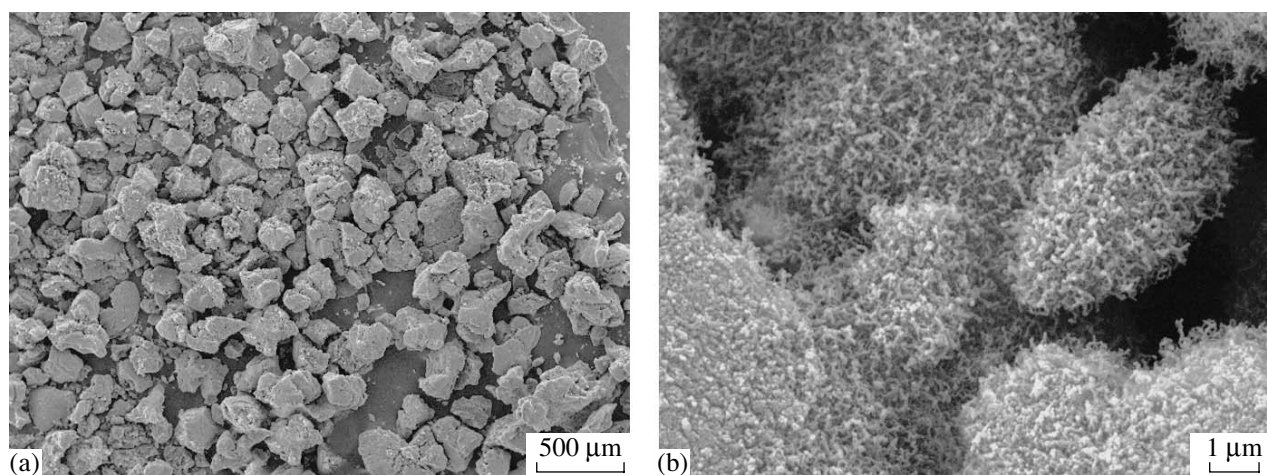
(a) 500 μm (b) 1 μm

Fig. 2. SEM micrographs of the surfaces of N-CNF samples prepared by the decomposition of a 50% C_2H_4–50% NH_3 mixture on the 65Ni–25Cu–Al_2O_3 catalyst at 550°C.

Physicochemical Characterization Techniques

The phase composition and structure properties of carbon materials were studied using ex situ X-ray diffraction (XRD) analysis. The X-ray diffraction patterns were measured on an HZG-4 diffractometer with monochromated CuK_α irradiation.

The structure and morphology of N-CNFs and N-AMCMs were studied using transmission electron microscopy (TEM). The samples were supported onto a holey carbon film on a copper grid. The TEM images were obtained on a JEM-2010 transmission electron microscope with a lattice resolution of 1.4 Å and an accelerating voltage of 200 kV. The surface morphology of N-CNFs was studied using scanning electron microscopy (SEM) on a JSM-6460 microscope at an accelerating voltage of 20 kV.

The texture characteristics of carbon materials were determined using the low-temperature adsorption of nitrogen at 77 K on an ASAP-2400 automated instrument. The specific surface area was calculated from the BET equation.

The nitrogen contents of carbon samples were determined using elemental analysis on a Carlo Erba Model 1106 automatic elemental analyzer.

The surface composition and the electronic states of nitrogen and carbon atoms in N-CNFs and N-AMCMs were studied using XPS. The measurements were performed on a VG ESCALAB HP photoelectron spectrometer with the use of AlK_α irradiation; the spectrometer was calibrated using the following lines: Au4f(7/2) = 84.0 eV, Ag3d(5/2) = 368.3 eV, and Cu2p(3/2) = 932.7 eV. The residual gas pressure in the measurements was no higher than 3×10^{-8} mbar.

RESULTS AND DISCUSSION

Synthesis and Properties of N-CNFs

It is well known that the amount of carbon formed in the decomposition of hydrocarbons is proportional to the metal content of the initial catalyst [11, 12, 32]. Therefore, it is reasonable to use high-percentage metal catalysts with metal concentrations of 70–90 wt % in order to prepare a carbon material in a high yield. Data given in Table 1 indicate that iron-containing catalysts exhibited low activity in the decomposition of a mixture of C_2H_4 and NH_3, whereas the 90Ni–Al_2O_3, 82Ni–8Cu–Al_2O_3, 65Ni–25Cu–Al_2O_3, 45Ni–45Cu–Al_2O_3, 75Co–Al_2O_3, and 72Co–3Mo–Al_2O_3 catalysts exhibited similar activity in terms of the yield of a carbon product and resulted in the formation of 11–14 g_C/g_{Cat}
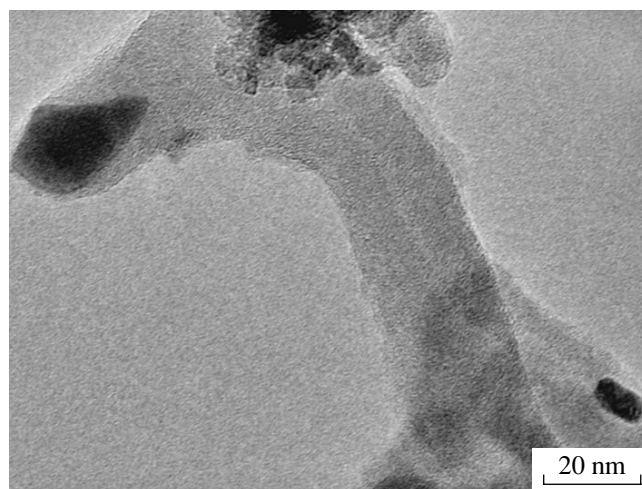

20 nm

Fig. 3. TEM micrograph of an N-CNF sample prepared by the decomposition of a C_2H_4–NH_3 mixture on the 65Ni–25Cu–Al_2O_3 catalyst: the internal structure of carbon fiber.
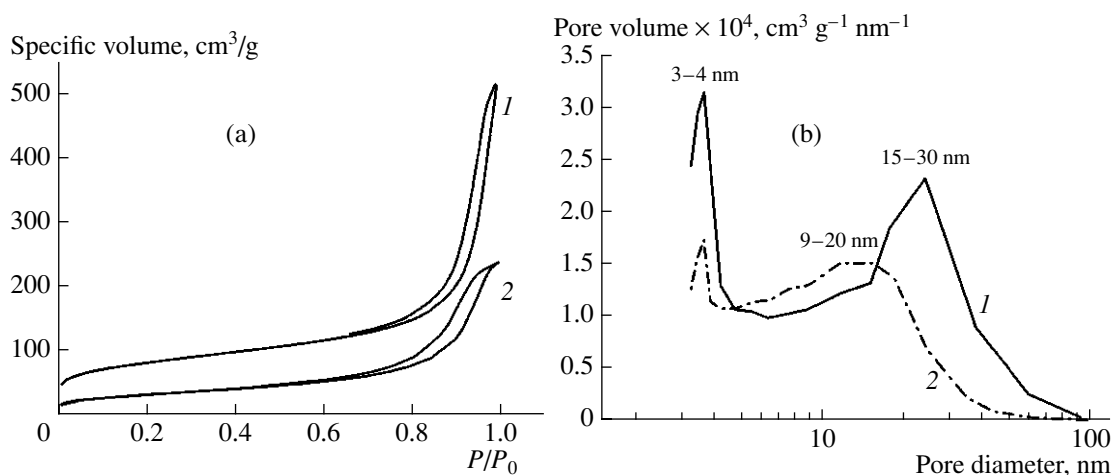
Fig. 4. (a) Sorption isotherms of N_2 at 77 K and (b) pore size distributions for N-CNF samples synthesized from a gas mixture of 50% C_2H_4 and 50% NH_3 for (1) 1 and (2) 20 h.

upon the decomposition of a 75% C_2H_4–25% NH_3 mixture for 1 h at 550–600°C. The maximum nitrogen content of N-CNFs and the maximum specific surface area were obtained with the use of the 65Ni–25Cu–Al_2O_3 catalyst. Therefore, this catalyst was chosen in order to perform a more detailed study of the formation of N-CNFs from a mixture of C_2H_4 and NH_3.

According to SEM data (Fig. 2a), a carbon material prepared by the decomposition of a mixture of C_2H_4 and NH_3 on the 65Ni–25Cu–Al_2O_3 catalyst consisting of granules of size 150–350 μm. As can be seen in high-resolution SEM micrographs (Fig. 2b), the surface of granules exhibited a fibrous morphology. Moreover, large pores about several micrometers in size were

Fig. 5. Dependence of the specific surface area of CNFs on the composition of the initial reaction mixture: (1) 75% C_2H_4 and 25% NH_3 or (2) 100% C_2H_4. $T = 550$°C.

observed. It is likely that each granule was a combination of several agglomerates; in turn, these agglomerates were formed by chaotically interwoven CNFs.

According to TEM data, CNFs are helical with a coaxial conical packing of graphite layers (Fig. 3); the fiber diameter is 25–100 nm. The XRD analysis of N-CNFs demonstrated that this material is graphite-like. The interplanar spacing varied within the range 0.343–0.347 nm depending on synthesis conditions. These values are higher than the interplanar spacing of ideal graphite (0.335 nm) [33]; this suggests the turbostratic structure of N-CNFs. With the use of XRD analysis, it was found that the size of coherent scattering regions of N-CNFs lies in the range 3.2–7.0 nm and is comparable with the size of coherent scattering regions for unmodified CNFs (3.3–9.5 nm) [14].

According to data on the low-temperature adsorption of N_2, the N-CNFs are mainly mesoporous materials, as evidenced by the type H1 capillary condensation hysteresis according to the IUPAC classification [34] (Fig. 4a). The BET average pore size was 5–19 nm. The specific surface area (S_{BET}) depended on CNF synthesis conditions and varied from 30 to 350 m^2/g. The pore size distribution curves had two maxima in the regions of 3–4 and 10–30 nm (Fig. 4b). Fenelonov et al. [35, 36] believed that pores of size 3–4 nm resulted from the formation of curved graphene structures on the closure of edge graphite planes at the fiber surface, whereas large pores of size 10–30 nm were spaces formed by the interweaving of fibers in the course of fiber growth. As the N-CNF synthesis time was increased, a distribution maximum in the region of large pores shifted toward smaller sizes. At the same time, the total pore volume decreased by a factor of 2 from 0.34–0.82 to 0.02–0.37 cm^3/g depending on the process temperature. It was found that the time dependence of S_{BET} exhibited a maximum in the region of 1–3 h at all of the reaction temperatures examined; in this case, lower synthesis
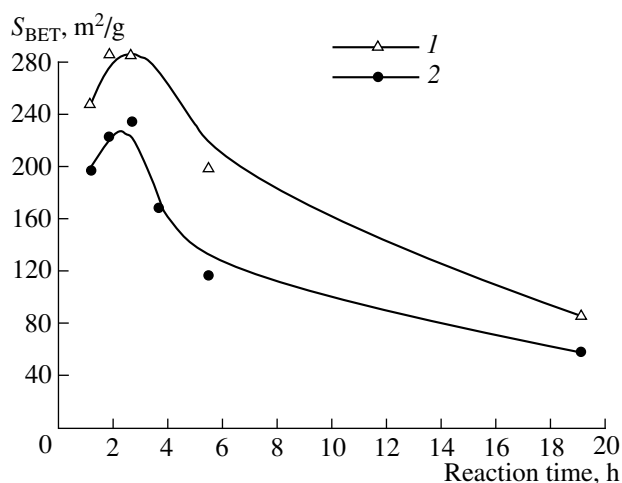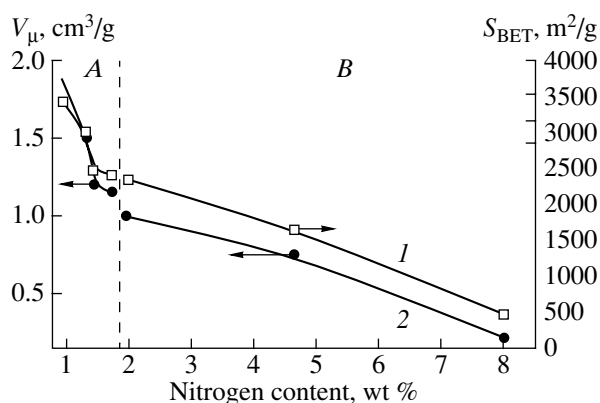
Fig. 6. Dependence of (*1*) specific surface area and (*2*) micropore volume on the nitrogen content of N-AMCM samples prepared with the use of (*A*) 8-hydroxyquinoline with benzotriazole or (*B*) *ortho*-nitroaniline with benzotriazole as precursors.
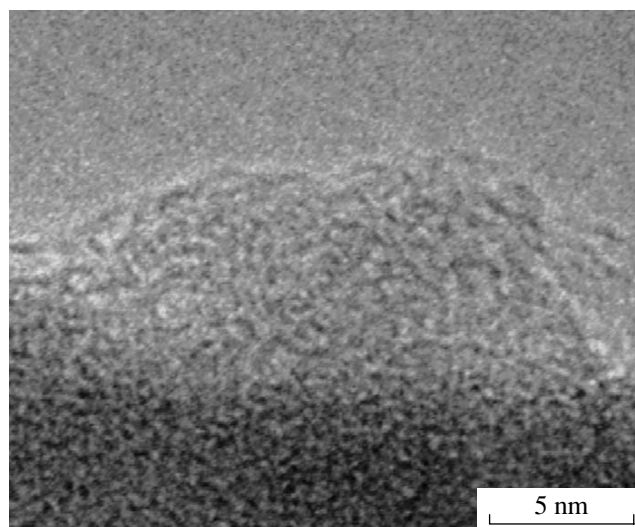

Fig. 7. TEM micrograph of an N-AMCM sample prepared from a mixture of *ortho*-nitroaniline and 8-hydroxyquinoline at 700°C (Table 3, sample no. 9).

temperatures were favorable for the production of higher specific surface areas. The dependence of S_{BET} on reaction time was also analogous for CNFs formed from 100% C_2H_4 (Fig. 5). Data shown in Fig. 5 indicate that the value of S_{BET} increased by a factor of 1.2–1.8 on the addition of ammonia to ethylene; in this case, the total pore volume increased by a factor of 1.1–1.6 and the micropore volume increased by a factor of 2.6–5.7 depending on reaction time.

A study of the effect of synthesis conditions on the nitrogen content of N-CNFs demonstrated that an increase in the reaction temperature from 550 to 675°C and an increase in the reaction time from 1 to 20 h resulted in a decrease in the nitrogen content of N-CNFs, whereas the nitrogen content of N-CNFs increased from 1.27 to 7.00 wt % as the concentration of ammonia in the reaction mixture was increased from 25 to 75 vol % (Table 2).

Synthesis and Properties of N-AMCMs

In the development of a preparation procedure for high-surface-area N-AMCMs with high nitrogen contents, we found that an increase in the alkali-to-precursor ratio, as well as an increase in the temperature and time of carbonization, resulted in an increase in the specific surface area and micropore volume of the resulting materials (Table 3). However, the severe conditions of carbonization resulted in a decrease in the nitrogen content of N-AMCMs to 1–2 wt % (sample nos. 3–7 and 9 in Table 3). It can be seen in Table 3 that milder carbonization conditions (700°C, a carbonization time of <40 min, and an alkali-to-precursor ratio of <2) were required for preparing N-AMCMs with a high nitrogen content. Under these conditions, we managed to obtain N-AMCMs with a nitrogen content of 4–8 wt % and a specific surface area of 472–1643 m²/g. Based on the experimental data, we found a correlation between texture characteristics and nitrogen concentration in N-AMCMs: an increase in the texture parameters

Table 2. Effect of synthetic conditions on the properties of N-CNFs

Precursor	T, °C	Time, h	N, wt %	Texture			
				S_{BET}, m²/g	S_{μ}^{*}, m²/g	V_{pore}, cm³/g	V_{μ}^{*}, cm³/g
75% C_2H_4/25% NH_3	550	1	1.58	282	33	0.51	0.02
75% C_2H_4/25% NH_3	675	1	1.27	199	0	0.31	0
50% C_2H_4/50% NH_3	550	1	3.13	287	32	0.82	0.02
50% C_2H_4/50% NH_3	550	20	2.44	112	0	0.37	0
25% C_2H_4/75% NH_3	550	1	7.00	191	0	0.71	0

* Micropore characteristics.

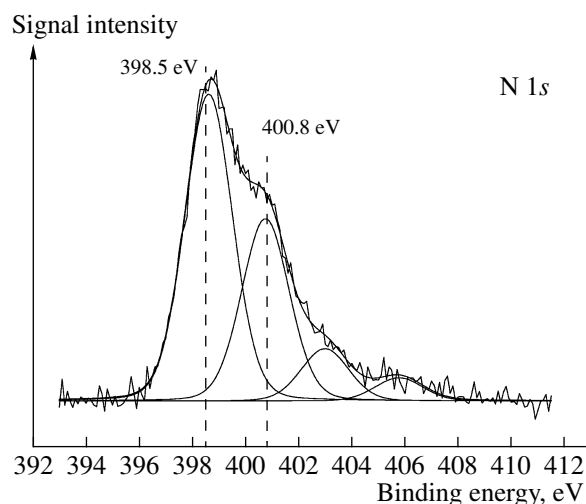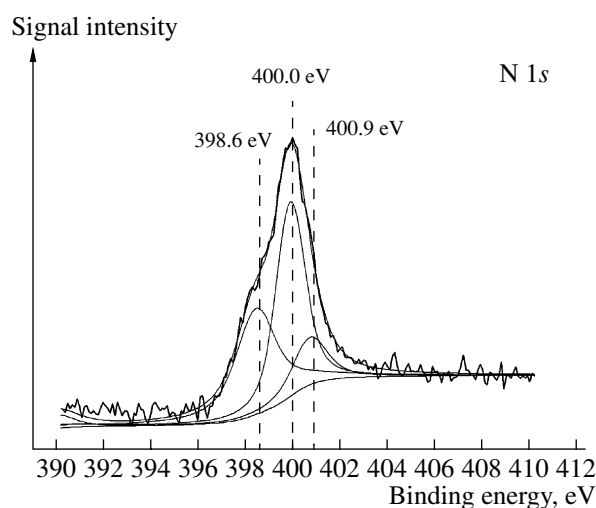**Table 3.** Effect of synthetic conditions on the properties of N-AMCMs

Sample no.	Precursor	NaOH/precursor, g/g	T, °C	Time, min	N, wt %	Texture			
						S_{BET}, m²/g	S_μ, m²/g	V_{pore}, cm³/g	V_μ, cm³/g
1	*ortho*-nitroaniline/1,2,3-benzotriazole	1.25	700	20	8.02	472	465	0.25	0.22
2		1.50	700	25	4.66	1643	1588	0.81	0.75
3		2.50	700	25	1.94	2352	1766	1.59	1.00
4	8-hydroxyquinoline/1,2,3-benzotriazole	1.75	700	45	1.74	2401	2242	1.31	1.14
5		2.00	900	25	1.42	2458	2418	1.24	1.20
6		2.50	700	80	0.92	3436	3183	2.16	1.88
7		3.00	700	30	1.47	3002	2536	1.97	1.50
8	*ortho*-nitroaniline/8-hydroxyquinoline	1.55	700	35	5.29	840	840	0.40	0.40
9		2.00	700	30	2.11	2559	2507	1.42	1.26

(S_{BET} and micropore volume) was accompanied by a decrease in the nitrogen content (Fig. 6). Nevertheless, the synthetic procedure developed allowed us to prepare N-AMCMs with a nitrogen content of 8 wt % and a sufficiently high specific surface area of 472 m²/g.

Figure 7 shows the TEM micrograph of an N-AMCM sample with a nitrogen content of 2.11 wt % and S_{BET} = 2559 m²/g. This sample was prepared by the carbonization of an equimolar mixture of *ortho*-nitroaniline and 8-hydroxyquinoline (Table 3, sample no. 9). According to TEM data, the structure of the N-AMCM consisted of curved graphite layers arranged at a distance of ~1 nm from each other, and it was identical to the structure of AMCMs free of bound nitrogen [15, 16].

State of Nitrogen in Carbon Materials

Based on an analysis of the XPS spectra of N-CNFs, we can conclude that at least two states of nitrogen with binding energies (BE) of 398.5 and 400.8 eV occurred in N-CNFs (Fig. 8). According to published data, a line with BE = 398.5 eV belongs to pyridinic nitrogen (N_{Py}) [37–39], whereas the N1*s* line with BE = 400.4–400.9 eV belongs to quaternary nitrogen (N_Q), that is, nitrogen atoms with a formal charge of +1, which replaced carbon atoms in the graphite plane and constituted an extended aromatic structure [38, 39]. The ratio between nitrogen species N_{Py}/N_Q in N-CNFs depended on the ammonia content of the starting mixture. As the concentration of ammonia in the reaction mixture was increased and, correspondingly, as the nitrogen content of N-CNFs increased, the fraction of pyridinic nitrogen

Fig. 8. XPS spectrum of N-CNF with a nitrogen content of 7.00 wt %.

Fig. 9. XPS spectrum of an N-AMCM sample with a nitrogen content of 5.29 wt % (Table 3, sample no. 8).

increased. The N_{Py}/N_Q ratio increased from 1.1 at 1 wt % to 1.7 at 7 wt % nitrogen in N-CNFs.

Figure 9 shows the N 1*s* spectrum of an N-AMCM sample with a nitrogen content of 5.29 wt % (Table 3, sample no. 8). An analysis of the XPS spectra of N-AMCMs allowed us to detect three electronic states of nitrogen atoms with binding energies of 398.6, 400.0, and 400.9 eV. Two signals, a more intense signal at 398.6 eV and a less intense signal at 400.9 eV, were analogous to the N 1*s* signals in the spectra of N-CNFs (Fig. 9). According to published data, an additional peak at 400.0 eV can be attributed to nitrogen atoms as the constituents of amino [40, 41], nitrile [41], or nitroso groups [39] bound to the graphite framework of a carbon material.

CONCLUSIONS

The study of the formation of nitrogen-containing carbon supports by the catalytic decomposition of a C_2H_4/NH_3 mixture and the carbonization of nitrogen-containing organic precursors allowed us to find the following regularities: The catalytic synthesis resulted in the production of a mesoporous material formed by chaotically interwoven structured CNFs. The carbonization of organic compounds produced AMCMs with high specific surface areas (to 3436 m^2/g). The nitrogen content of these materials depended only on synthetic conditions. An increase in the process temperature and time resulted in a decrease in the nitrogen contents of N-CNFs and N-AMCMs. An increase in the nitrogen content of a precursor (the concentration of ammonia in a C_2H_4/NH_3 mixture or the number of nitrogen atoms in an organic compound) was accompanied by an increase in the nitrogen content of carbon materials. As a result, nitrogen-containing carbon supports with nitrogen contents to 8 wt % could be prepared.

We found that nitrogen atoms as the constituents of carbon materials can occur in various electronic states. The following two main nitrogen species as the constituents of N-CNFs were detected: pyridinic (398.5 eV) and quaternary nitrogen (400.8 eV). The electronic state distribution of nitrogen atoms depended on the total nitrogen content of N-CNFs; the contribution of the pyridinic component increased as the total nitrogen content was increased. An additional state of nitrogen atoms (400.0 eV), which could be interpreted as the nitrogen constituent of nitroso groups, was observed in the case of amorphous microporous materials.

The dependence of the texture properties of N-CNFs on synthetic conditions was directly opposite to that of N-AMCMs. Thus, milder process conditions (low temperatures and short-time synthesis) resulted in a larger surface area of N-CNFs. Higher carbonization temperatures and longer process times facilitated the formation of high-surface-area N-AMCMs with large micropore volumes.

Thus, the developed approaches to the synthesis of nitrogen-containing carbon supports can be used for the preparation of a wide range of carbon materials structurally modified with nitrogen. In this case, the properties of the materials synthesized depend on preparation conditions, and they can be varied over a wide range. This provides opportunities to perform the target-oriented synthesis of nitrogen-containing carbon supports for electrocatalysts with specified properties.

REFERENCES

1. Gottesfeld, S. and Zawodzinski, T.A., *Adv. Electrochem. Sci. Eng.*, 1997, vol. 5, p. 195.

2. Gasteiger, H.A., Kocha, Sh.S., Sompalli, B., and Wagner, F.T., *Appl. Catal., B*, 2005, vol. 56, p. 9.

3. Thompson, S.D., Jordan, L.R., and Forsyth, M., *Electrochim. Acta*, 2001, vol. 46, p. 1657.

4. Ralph, T.R. and Hogarth, M.P., *Platinum Met. Rev.*, 2002, vol. 46, p. 3.

5. Bessel, C.A., Laubernds, K., Rodrigues, N.M., and Baker, R.T.K., *J. Phys. Chem. B*, 2001, vol. 105, no. 6, p. 1115.

6. Matsumoto, T., Komatsu, T., Nakano, H., Arai, K., Nagashima, Y., Yoo, E., Yamazaki, T., Kijima, M., Shimizu, H., Takasawa, Y., and Nakamura, J., *Catal. Today*, 2004, vol. 90, p. 277.

7. Gangeri, M. and Centi, G., La Malfa A., Perathoner S., Vieira R., Pham-Huu C., Ledoux M.J, *Catal. Today*, 2005, vols. 102–103, p. 50.

8. Ismagilov, Z.R., Kerzhentsev, M.A., Shikina, N.V., Lisitsyn, A.S., Okhlopkova, L.B., Barnakov, Ch.N., Sakashita, M., Iijima, T., and Tadokoro, K., *Catal. Today*, 2005, vols. 102–103, p. 58.

9. Serp, Ph., Corrias, M., and Kalck, Ph., *Appl. Catal., A*, 2003, vol. 253, p. 337.

10. De Jong, K.P. and Geus, J.W., *Catal. Rev. Sci. Eng.*, 2000, vol. 42, no. 4, p. 481.

11. Avdeeva, L.B., Reshetenko, T.V., Ismagilov, Z.R., and Likholobov, V.A., *Appl. Catal., A*, 2002, vol. 228, nos. 1–2, p. 53.

12. Avdeeva, L.B., Kochubey, D.I., and Shaikhutdinov, Sh.K., *Appl. Catal., A*, 1999, vol. 177, p. 43.

13. Shaikhutdinov, Sh.K., Zaikovskii, V.I., and Avdeeva, L.B., *Appl. Catal., A*, 1996, vol. 148, p. 123.

14. Reshetenko, T.V., Avdeeva, L.B., Ismagilov, Z.R., Push-karev, V.V., Cherepanova, S.V., Chuvilin, A.L., and Likholobov, V.A., *Carbon*, 2003, vol. 41, p. 1605.

15. RF Patent 2 206 394, 2003.

16. Barnakov, Ch.N., Kozlov, A.P., Seit-Ablaeva, S.K., Fenelonov, V.B., Cherepanova, S.R., Ismagilov, Z.R., and Parmon, V.N., *Neftekhimiya*, 2004, no. 6, p. 436 [*Pet. Chem.* (Engl. Transl.), no. 6, p. 403].

17. Barnakov, Ch.N., Kozlov, A.P., Seit-Ablaeva, S.K., Romanenko, A.I., Vasenin, N.T., Anufrienko, V.F., Ismagilov, Z.R., and Parmon, V.N., *Ross. Khim. Zh.*, 2006, vol. 50, no. 1, p. 54.

18. Japanese Patent 2005135817, 2005.

19. Maiyalagan, T., Viswanathan, B., and Varadaraju, U.V., *Electrochem. Commun.*, 2005, vol. 7, p. 905.

20. Miyamoto, Y., Cohen, M.L., and Louie, S.G., *Solid State Commun.*, 1997, vol. 102, no. 8, p. 605.

21. Golberg, D., Dorozhkin, P.S., Bando, Y., Dong, Z.-C., Tang, C.C., Uemura, Y., Grobert, N., Reyes-Reyes, M., Terrones, H., and Terrones, M., *Appl. Phys. A*, 2003, vol. 76, p. 499.

22. Bron, M., Radnik, J., Fieber-Erdmann, M., Bogdanoff, P., and Fiechter, S., *J. Electroanal. Chem.*, 2002, vol. 535, p. 113.

23. Jasinski, R., *Nature*, 1964, vol. 201, p. 1212.

24. Jahnke, H., Schonborn, M., and Zimmermann, G., *Top. Curr. Chem.*, 1976, vol. 61, p. 133.

25. Van Veen, J.A.R., Colijn, H.A., and van Baar, J.F., *Electrochim. Acta*, 1988, vol. 33, p. 801.

26. Van Wingerden, B., van Veen, J.A.R., and Mensch, C.T.J., *J. Chem. Soc., Faraday Trans.*, 1988, vol. 84, p. 65.

27. Lalande, G., Côté, R., Tamizhmani, G., Guay, D., Dode-let, J.P., Dignard-Bailey, L., Weng, L.T., and Bertrand, P., *Electrochim. Acta*, 1995, vol. 40, p. 2635.

28. Tamizhmani, G., Dodelet, J.P., Guay, D., and Capuano, G., *J. Electrochem. Soc.*, 1994, vol. 141, p. 41.

29. Faubert, G., Cote, R., Dodelet, J.P., Lefevre, M., and Bertrand, P., *Electrochim. Acta*, 1999, vol. 44, p. 2589.

30. Wei, G., Wainright, J.S., and Savinell, R.F., *J. New Mater. Electrochem. Syst.*, 2000, vol. 3, p. 121.

31. Shaikhutdinov, Sh.K., Avdeeva, L.B., Goncharova, O.V., Kochubey, D.I., Novgorodov, B.N., and Plyasova, L.M., *Appl. Catal., A*, 1995, vol. 126, p. 125.

32. Reshetenko, T.V., Avdeeva, L.B., Ushakov, V.A., Moroz, E.M., Shmakov, A.N., Kriventsov, V.V., Kochubey, D.I., Pavlyukhin, Yu.T., Chuvilin, A.L., and Ismagilov, Z.R., *Appl. Catal., A*, 2004, vol. 270, p. 87.

33. Hishiyama, Y. and Nakamura, M., *Carbon*, 1995, vol. 33, no. 10, p. 1399.

34. Gregg, S.J. and Sing, K.S.W., *Adsorption, Surface Area, and Porosity*, London: Academic, 1967.

35. Fenelonov, V.B., Avdeeva, L.B., Zheivot, V.I., Okkel', L.G., Goncharova, O.V., and Pimneva, L.G., *Kinet. Katal.*, 1993, vol. 34, no. 3, p. 545.

36. Fenelonov, V.B., Derevyankin, A.Yu., Okkel, L.G., Avdeeva, L.B., Zaikovskii, V.I., Moroz, E.M., Salanov, A.N., Rudina, N.A., Likholobov, V.A., and Shaikhutdinov, Sh.K., *Carbon*, 1997, vol. 35, no. 8, p. 1129.

37. Kvon, R.I., Il'inich, G.N., Chuvilin, A.L., and Likholobov, V.A., *J. Mol. Catal. A*, 2000, vol. 158, p. 413.

38. Kim, T.-Y., Lee, K.-R., Eun, K.Y., and Oh, K.-H., *Chem. Phys. Lett.*, 2003, vol. 372, p. 603.

39. Pels, J.R., Kapteijn, F., Moulijn, J.A., Zhu, Q., and Thomas, K.M., *Carbon*, 1995, vol. 33, no. 11, p. 1641.

40. Seno, M., Tsuchiya, Sh., and Ogawa, Sh., *J. Am. Chem. Soc.*, 1977, vol. 99, no. 9, p. 3014.

41. Riedo, E., Comin, F., Chevrier, J., and Bonnot, A.M., *J. Appl. Phys.*, 2000, vol. 88, no. 7, p. 4365.